



Contents lists available at ScienceDirect

Bioorganic & Medicinal Chemistry Letters

journal homepage: www.elsevier.com/locate/bmcl



Potent inhibitors of Huntingtin protein aggregation in a cell-based assay

Alison Rinderspacher^a, Maria Laura Cremona^b, Yidong Liu^a, Shi-Xian Deng^a, Yuli Xie^a, Gangli Gong^a, Nathalie Aulner^b, Udo Többen^b, Katherine Myers^b, Caty Chung^c, Monique Andersen^d, Dušica Vidović^c, Stephan Schürer^c, Lars Brandén^b, Ai Yamamoto^d, Donald W. Landry^{a,*}

^a Division of Experimental Therapeutics, Department of Medicine, Columbia University, 630 West 168th Street, New York, NY 10032, USA

^b Genome Center, Columbia University, 1150 St. Nicholas Ave., New York, NY 10032, USA

^c Scientific Computing, The Scripps Research Institute, 5353 Parkside Drive, Jupiter, FL 33458, USA

^d Department of Neurology, Columbia University, 630 West 168th Street, New York, NY 10032, USA

ARTICLE INFO

Article history:

Received 18 December 2008

Revised 24 January 2009

Accepted 27 January 2009

Available online 30 January 2009

Keywords:

Huntington's disease

Huntingtin protein

Polyglutamine aggregates

Inhibitors of huntingtin protein aggregation

High-throughput screen

Quinazoline

ABSTRACT

A quinazoline that decreases polyglutamine aggregate burden in a cell-based assay was identified from a high-throughput screen of a chemical-compound library, provided by the NIH Molecular Libraries Small Molecule Repository (MLSMR). A structure and activity study yielded leads with submicromolar potency.

© 2009 Elsevier Ltd. All rights reserved.

Huntington's disease (HD), a member of the trinucleotide-repeat neurological disorders, is caused by a heritable, polyglutamine-expansion mutation in the NH3-terminus of the Huntingtin protein (Htt).^{1–3} The intracellular accumulation of insoluble aggregates of mutant Htt is a hallmark of HD, but the precise mechanism of toxicity remains a matter of conjecture.⁴ In mouse models of HD, expression of the NH3-terminal portion of the mutant Htt protein recapitulates key features of the disease with mice displaying a phenotype of progressive neurological impairment. Neurons in these models^{5,6} show an intrinsic ability to clear polyQ aggregates, and accompanying this clearance, a reversal of the HD-like neurologic symptoms is observed. Macroautophagy, the lysosome-mediated degradation of cytosolic proteins, is implicated as the cellular pathway responsible for aggregate clearance.^{7–10} Using a unique two-tiered functional genetic screen, we previously found that macroautophagy-mediated clearance of accumulated mutant protein can be increased through IRS-2 stimulation in a cell-based model of HD.⁷ In order to search for small-molecule activators of Htt clearance, we used this model in a high-throughput fluorescent cell-based assay format to monitor the aggregation and clearance of a tet-regulatable,¹¹ conditionally expressed mutant protein consisting of the first 17 NH3-terminal amino acids of Htt followed by

a polyQ stretch of 103 residues fused to a monomeric cyan fluorescent protein (mCFP).⁷ These stable transfectants do not manifest the acute polyQ-length-dependent cell death observed after transient transfection⁷ and thus provided an excellent platform for the identification of modulators of protein degradation which act over a period of days.

The degree of aggregation in this assay is measured by the presence and magnitude of fluorescent intracellular inclusions. We screened a 10K chemical-compound library, provided by the NIH-sponsored MLSCN, for diminution of aggregation of mutant protein after incubation for 72 h. We identified six hits: five tetracycline derivatives, likely suppressing tet-regulatable gene expression, and quinazoline **1a** (Fig. 1), with an IC₅₀ of approximately

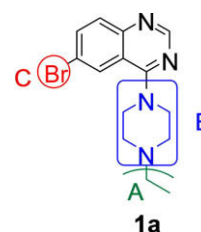
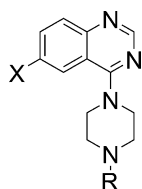


Figure 1. Structure analysis of our lead compound.

* Corresponding author. Tel.: +1 212 305 5838; fax: +1 212 305 3475.

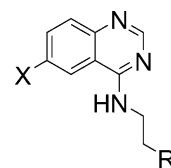
E-mail address: dwl1@columbia.edu (D.W. Landry).

Table 1
Modifications of regions A and C: IC₅₀ values of our piperazine analogs **1–4**

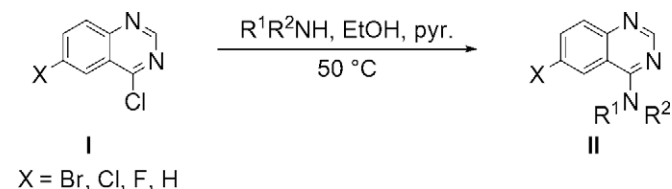


Compound	X	R	IC ₅₀ , μM
1a	Br	Ethyl	2.21
1b	Cl	Ethyl	3.63
1c	F	Ethyl	5.26
1d	H	Ethyl	>10
2a	Br	Methyl	1.31
2b	Cl	Methyl	>10
2c	F	Methyl	>10
2d	H	Methyl	>10
3a	Br	H	2.74
4a	Br	4-(1,3-Benzodioxol-5-ylmethyl)	Inactive
4b	Cl	4-(1,3-Benzodioxol-5-ylmethyl)	1.07
4c	F	4-(1,3-Benzodioxol-5-ylmethyl)	>10
4d	H	4-(1,3-Benzodioxol-5-ylmethyl)	>10

Table 2
Modifications of regions B and C: IC₅₀ values of our secondary amine analogs **5–11**



Compound	X	R	IC ₅₀ , μM
5a	Br	Phenol	1.11
5b	Cl	Phenol	0.71
5c	F	Phenol	6.38
5d	H	Phenol	>15.8
6a	Br	4-Chlorophenyl	Inactive
6b	Cl	4-Chlorophenyl	3.44
6c	F	4-Chlorophenyl	Inactive
6d	H	4-Chlorophenyl	10.5
7	Cl	4-Phenoxyphenyl	Inactive
8	NH ₂	4-Phenoxyphenyl	Inactive
9	Cl	4-(Cyclopentyloxy)phenyl	Inactive
10	Cl	4-(Benzyloxy)phenyl	Inactive
11	Cl	Ethyl (4-phenoxy)acetate	4.48

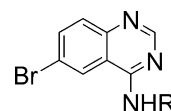


Scheme 1. General procedure for the synthesis of our quinazoline compounds.

4 μM. The structure of **1a** was confirmed by synthesis and dose-dependent activity was demonstrated with an IC₅₀ of 2.2 μM (Table 1). A structure–activity relationship (SAR) study was conducted to identify more potent derivatives. Three regions of the quinazoline were selected for modification: A, the distal piperazine N-alkyl group; B, the piperazine ring itself; and C, the 6-bromo group on the aromatic core. We envisioned that analogs would be easily synthesized from common 4-chloro-6-halo-quinazoline intermediates (Scheme 1).¹² As this work proceeded, Sarkar et al., seeking enhancers of autophagy, reported several bromo-substituted quinazolines¹³ and we synthesized three of their compounds, **12–14**, for comparison (Table 3).

Substitution at the N-ethyl group of quinazoline **1a** with either smaller or bulkier groups did not alter activity (Table 1). In contrast, substitution at the 6-position with fluorine or hydrogen was not well tolerated compared to substitution with bromine or chlorine. This pattern for substitution at the 6-position was also observed in the series based on replacement of the piperazine ring with 4'-substituted phenylethylene amine. That is, the activity of the 6-fluoro- and dehalogenated derivatives was generally lower (Table 2). In general, the secondary amines of Table 2 were superior to the corresponding piperazines of Table 1. Quinazoline itself is inactive in our assay and any substitutions of the quinazoline core with other cores resulted in loss of activity. Substitution of the amino group with an alkoxy group also resulted in loss of activity. The most potent inhibitor of accumulation of aggregated mutant Htt fragment was compound **5b** with an IC₅₀ of 0.71 μM. Alkylation of the 4'-hydroxyl group of compound **5b** was not tolerated, cf compounds **7–10**.

Table 3
Quinazoline derivatives **12–14** of Sarkar et al.: IC₅₀ values in our assay



Compound	R	IC ₅₀ , μM
12	Propyl	8.13
13	Allyl	5.36
14	Benzyl	6.13

Sarkar compounds **12–14** were reported to have EC₅₀ values of approximately 50 μM in a yeast assay. While no rank order was reported for this assay, the potency of the compounds in PC12 cells was **12** > **13** > **14** and in COS-7 cells was **14** > **13** > **12**.¹³ In contrast, we found low micromolar potency in our system with a rank order of **12** > **14** > **13** (Table 3). It remains to be formally demonstrated that our assay and that of Sarkar et al. are directed to the same target.

The decrease in the number of aggregates per cell observed with our compound may be due to the clearance of inclusions because the number of inclusions after the administration of compounds such as **5b** is less than the number before treatment. Nonetheless, other factors may be at play, such as enhanced cell division leading to cytoplasmic dilution, and thus an apparent decrease in the number of inclusions, or enhanced cell death leading to a preferential loss of aggregate-containing cells. To eliminate these possibilities, we examined cell numbers and cell death after administration of compound **5b**. As shown in Figure 2, despite the clearance of inclusions, neither signs of cytotoxicity nor differences in the total number of cells were observed.

In summary, we prepared and identified four potent inhibitors of Huntingtin protein aggregation, **5b**, **4b**, **5a**, and **2a**. Our library of analogs provides a starting point for mechanistic studies to determine the target of action.

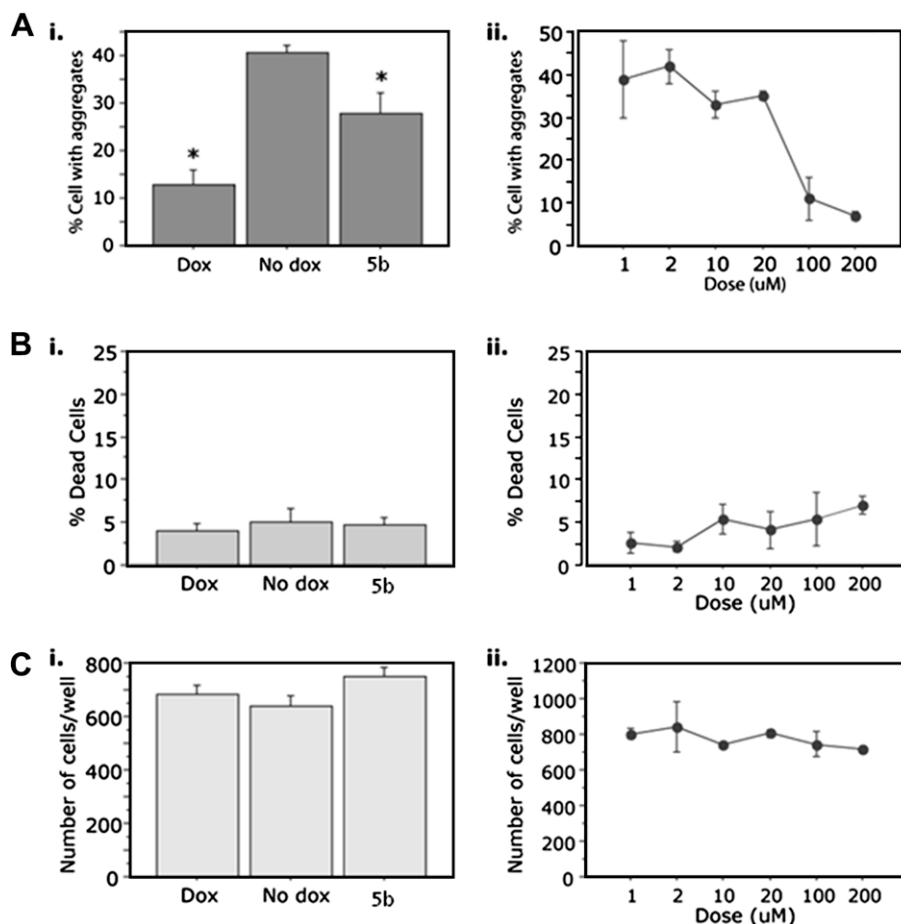


Figure 2. Compound **5b** leads to a dose-dependent decrease in the number of aggregates per cell in the absence of increased proliferation or cell death. Cells were seeded in a 96-well format and treated with 2 $\mu\text{g}/\text{mL}$ doxycycline (Dox), 0.1% DMSO (No Dox) as control, or compound **5b**. (A) Percent (%) cells with aggregates. (i) The overall effect of **5b** on % cells with aggregates with respect to Dox and No Dox. ANOVA reveals a statistically significant effect of 'Treatment' on '% Cells with aggregates' ($F(2,37) = 14.486$, $p < 0.001$, $p < 0.05$ in Fisher Post hoc analysis when compared to No Dox). (ii) **5b** exerts a dose-dependent decrease of aggregates. (B) % Dead cells. There is no effect on cell death of **5b** as compared to Dox or No Dox (i) or across dose (ii). ($F(2,37) = 0.346$; $p = 0.7095$). (C) Number of cells per well. There is no effect on the total cell number of **5b** as compared to Dox or No Dox (i) or across dose (ii). ($F(2,37) = 2.225$; $p = 0.1224$).

Acknowledgments

The authors would like to acknowledge Teresa Wojtasiewicz for technical support and would like to thank the NIH's Molecular Libraries Initiative for funding our research.

References and notes

- Zhang, X.; Smith, D. L.; Meriin, A. B.; Engemann, S.; Russel, D. E.; Roark, M.; Washington, S. L.; Maxwell, M. M.; Marsh, J. L.; Thompson, L. M.; Wanker, E. E.; Young, A. B.; Housman, D. E.; Bates, G. P.; Sherman, M. Y.; Kazantsev, A. G. *Proc. Natl. Acad. Sci. U.S.A.* **2005**, *102*, 892.
- Colby, D. W.; Chu, Y.; Cassady, J. P.; Duennwald, M.; Zazulak, H.; Webster, J. M.; Messer, A.; Lindquist, S.; Ingram, V. M.; Wittrup, K. D. *Proc. Natl. Acad. Sci. U.S.A.* **2004**, *101*, 17616.
- Heiser, V.; Scherzinger, E.; Boeddrich, A.; Nordhoff, E.; Lurz, R.; Schugardt, N.; Lehrach, H.; Wanker, E. E. *Proc. Natl. Acad. Sci. U.S.A.* **2000**, *97*, 6739.
- Arrasate, M.; Mitra, S.; Schweitzer, E. S.; Segal, M. R.; Finkbeiner, S. *Nature* **2004**, *431*, 805.
- Yamamoto, A.; Lucas, J. J.; Hen, R. *Cell* **2000**, *101*, 57.
- Mangiarini, L.; Sathasivam, K.; Seller, M.; Cozens, B.; Harper, A.; Hetherington, C.; Lawton, M.; Trotter, Y.; Lehrach, H.; Davies, S. W.; Bates, G. P. *Cell* **1996**, *87*, 493.
- Yamamoto, A.; Cremona, M. L.; Rothman, J. E. *J. Cell Biol.* **2006**, *172*, 719.
- Iwata, A.; Riley, B. E.; Johnston, J. A.; Kopito, R. R. *J. Biol. Chem.* **2005**, *280*, 40282.
- Iwata, A.; Christianson, J. C.; Bucci, M.; Ellerby, L. M.; Nukina, N.; Forno, L. S.; Kopito, R. R. *Proc. Natl. Acad. Sci. U.S.A.* **2005**, *102*, 13135.
- Filimonenko, M.; Stuffers, S.; Raiborg, C.; Yamamoto, A.; Malerød, L.; Fisher, E. M. C.; Isaacs, A.; Brech, A.; Stenmark, H.; Simonsen, A. *J. Cell Biol.* **2007**, *179*, 485.
- Gossen, M.; Bujard, H. *Annu. Rev. Genet.* **2002**, *36*, 153.
- ¹H NMR and ¹³C NMR spectra were recorded on a Varian Mercury 300 T NMR spectrometer. High-resolution mass spectrometry was done by Dr. Yasuhiro Itagaki at Columbia University. 4,6-Dichloroquinazoline (**1**, X = Cl) was stirred at room temperature in a 4:1 mixture of ethanol (4.0 mL) and pyridine (1.00 mL). Tyramine (0.124 g, 0.904 mmol) was added to the white suspension which immediately upon addition of the amine turned dark bright orange and then gradually turned into a clear, bright orange solution. The solution was stirred overnight and was subsequently heated for 5 h at 50 °C, after which it was allowed to cool to room temperature. The product was purified via column chromatography (1:1 hexanes: ethyl acetate) to give a white solid, **5b**. (0.106 g, 0.354 mmol, 59%); mp 178–180 °C; ¹H NMR (300 MHz, (CD₃)₂SO) δ 9.19 (s, 1H), 8.49 (s, 1H), 8.39 (s, 1H), 7.78 (d, 1H, $J = 9.0$ Hz), 7.69 (d, 1H, $J = 8.7$ Hz), 7.05 (d, 2H, $J = 8.1$ Hz), 6.68 (d, 2H, $J = 8.4$ Hz), 3.67 (t, 2H, $J = 7.5$ Hz), 2.83 (t, 2H, $J = 7.5$ Hz); ¹³C NMR (75 MHz, (CD₃)₂SO) δ 158.4 (1C), 155.5 (1C), 155.4 (1C), 147.6 (1C), 132.7 (1C), 129.6 (2C), 129.4 (2C), 129.3 (1C), 121.9 (1C), 115.7 (1C), 115.0 (2C), 42.6 (1C), 33.6 (1C); ESI-MS ($M^+ + H$): 300; FAB + HRMS calcd for C₁₆H₁₅ON₃ ³⁵Cl: 300.0904. Found: 300.0902; MS m/z 300 ($M^+ + H$, 100%), 235, 217, 192, 180, 176.
- Sarkar, S.; Perlstein, E. O.; Imarisio, S.; Pineau, S.; Cordenier, A.; Maglathlin, R. L.; Webster, J. A.; Lewis, T. A.; O' Kane, C. J.; Schreiber, S. L.; Rubinsztajn, D. C. *Nat. Chem. Biol.* **2007**, *3*, 331.